J. Water Environ. Nanotechnol., 7(3): 317-331 Summer 2022

ORIGINAL RESEARCH PAPER

Extraction and Characterization of Nanocellulose from Wheat Straw: Facile Approach

Savita Sihag[1], Sheetal[2], Monika Yadav[3], Jitender Pal*

[1] Savita Sihag, PhD Research Scholar, Department of Environmental Science and Engineering, Guru Jambheshwar University of Science and Technology, Hisar (Haryana), India
[2] Sheetal, PhD Research Scholar, Department of Environmental Science and Engineering, Guru Jambheshwar University of Science and Technology, Hisar (Haryana), India
[3] Monika Yadav, PhD Research Scholar, Department of Environmental Science and Engineering, Guru Jambheshwar University of Science and Technology, Hisar (Haryana), India
[4] Dr. Jitender Pal, Professor, Department of Environmental Science and Engineering, Guru Jambheshwar University of Science and Technology, Hisar (Haryana), India*

Received: 2022-04-04 Accepted: 2022-06-21 Published: 2022-07-01

ABSTRACT
The environmental concern occurs due to the extreme use of synthetic materials that have been fortified to develop innovative, multifunctional, and sustainable materials using copious lignocellulosic biomass. In this present study, work was done on the extraction of nanocellulose from wheat straw, and found that wheat straw is an admirable source of cellulose. Chemical processes were used to isolate the cellulose and remove unwanted lignin and hemicellulose from wheat straw followed by sonication, cryo-crushing, and magnetic stirring to achieve nanocellulose. The observed amount of cellulose (36.1%), hemicellulose (30.3%), lignin (17%), and ash content (9.2%) of raw wheat straw. Structural, morphological, and thermal characterization were estimated from FTIR, XRD, FESEM, TEM, DSC, TGA, and AFM for the identification and characterization of extracted cellulose from wheat straw. FTIR showed that the peaks at wavelength 1430.50 cm-1 and 1638.41 cm-1 both show that cellulose is present in the extracted nanocellulose. Extracted nanocellulose was crystalline and had a 68.96% Crystallinity Index. Morphological analysis, FESEM showed that the untreated wheat straw has an irregular porous structure but the extracted nanocellulose has a regular shape having straight fibers connected. TEM analysis showed that the extracted nanocellulose has a spherical shape structure connected, showing the regular shape, the obtained spherical shape regulates the nanocellulose for further applications. Thermal degradation was observed using TGA which shows that the nanocellulose decomposition was observed around 3600C. AFM determination shows a bell-shaped structure on a smooth surface with a particle height of 3.2 nm and the mean roughness of 110.4 nm was obtained from the extracted nanocellulose. Extracted nanocellulose has a particle size of 58.77 nm.

Keywords: *Wheat Straw, Acid Hydrolysis, Cryocrushing, Thermal analysis, Nanocellulose*

How to cite this article
Sihag S., Sheetal, Yadav M., Pal J. Extraction and Characterization of Nanocellulose from Wheat Straw: Facile Approach. J. Water Environ. Nanotechnol., 2022; 7(3): 317-331.
DOI: 10.22090/jwent.2022.03.007

INTRODUCTION

Wheat is one of the most common crops among the crops in India and more than 94 million tonnes of wheat are produced per year [1]. The main higher productivity state of wheat grown are Punjab, Haryana, Madhya Pradesh, and Uttar Pradesh. Billion tons of wheat crop residue wheat straw after harvesting have been left in the field. It is an easily available renewable source of lignocellulosic biomass. Wheat straw is an agricultural by-product of the wheat crop and is available in abundant in north India. The higher C-N content of wheat straw leads to lower bio-degradability in contrast to other

* Corresponding Author Email: *j_pal2k1@yahoo.com*

agricultural remains. A smaller amount of it is utilized for animal feed, the production of biogas and biofuel, and other industrial applications such as the extraction of cellulose and hemicellulose. However, most farmer prefers to burn wheat crop residues directly in the field because it is the cheapest and quiet method to manage crop residues [2], [3]. It is an important basis for worse air quality [4]. Blaze releases due to forest fire, owing to high carbon content levels [5]. Residues blazing release a higher extent of air pollutants such as N_2O, CO_2, CH_4, CO, SO_2, NH_4, HC, VOC_S and suspended particulate matter in varied ranges depending on the residual composition [6], [7]. The mentioned pollutants in the air cause hostile effects on human health. They can cause diseases to the skin, cataracts, pulmonary tuberculosis, pulmonary diseases, pneumoconiosis, eye irritation, bronchitis, and blindness. Road accident cases also increase throughout the stubble burning period.

Consequently, it is of major concern to grow economic and scientific methods for recovering cellulose from agricultural wastes. Lots of efforts have been made by various researchers and engineers to produce environmental-friendly composite constituents from agricultural wastes [8], [9], [10], [11], [12].

Cellulose shows excellent mechanical properties, such as high strength (2-6 GPA) and toughness [13] lower density, a high length-to-diameter ratio [2], [14], macroscopic quantum tunneling effect, surface effect and smaller size effect, low coefficient of thermal expansion [15], high Young's modulus (138 GPa) [16] biodegradability and biocompatibility, high availability as a renewable material, barrier properties, dimensional constancy. Presently, agricultural residue containing cellulosic materials that are green, maintainable, and environmentally approachable [17] has been extensively established for nanocellulose extraction [18], [19]. The exceptionality of nanocellulose elements depends on the characteristics of the material and methodology used in manufacturing [20]. Nanocellulose size generally has a diameter of 1-100 nm or lesser than that in a single dimension. Based on the extents, preparation methods and functions, nanocellulose is classified as cellulose nanofibers (CNF) [21],cellulose nanocrystals (CNC) [22], [23], [24] and biological nanocellulose.

The various methods used for the extraction of nanocellulose by the various researchers worldwide example, described in Table.1 were electrospinning [25], [26], [27], oxidation by reduction of the crystalline fibres in the nanosized units [28], [29], high pressure homogenization and refining [30], [31], [32], enzymatic hydrolysis [33], [34], cryo-crushing [35], [36], micro-fluidization [37], [38], [39], higher intensity ultrasonication [40], [41], [42], steam explosion [30], [43]. Amongst the various methodologies used in the preparation of nanocellulose, acid hydrolysis is the utmost protruding and widely used method [44], [45], [46], [47] that disintegrates amorphous segment and disordered cellulose which provides distinct crystals along with higher notch of crystallinity [48], [49], [50]. Extracted nanocellulose has wider applications in the field of environmental science/ engineering such as water treatment [51], energy as fuel cell applications [51], as an effective solar cell substrate [51] removal of dyes, heavy metals, fluoride [52], phytoremediation [53] and other areas such as drug delivery, food packaging, paint industry, etc.

On a structural and compositional basis, a stiff outer cover that shields the plant cell is called a cell wall. A cell wall is composed of three layers: middle lamella, primary wall, and secondary wall [54]. Middle lamella has a higher quantity of lignin and is mainly accountable for the binding of adjacent cells [55]. The primary wall is around 30–1000 nm thicker and has three main components-pectin,

Table 1. Nanocellulose Extraction Methods

Sr. No.	Extraction Method	References
1	Electrospinning	[25], [26], [27]
2	Oxidation by reduction	[28], [29]
3	High pressure homogenization and refining	[30], [31], [32]
4	Enzymatic hydrolysis	[33], [34]
5	Cryo-crushing	[35], [36]
6	Micro-fluidization	[37], [38], [39]
7	Higher intensity ultrasonication	[40], [41], [42]
8	Steam explosion	[30], [43]
9	Acid hydrolysis	[44], [45], [46], [47]

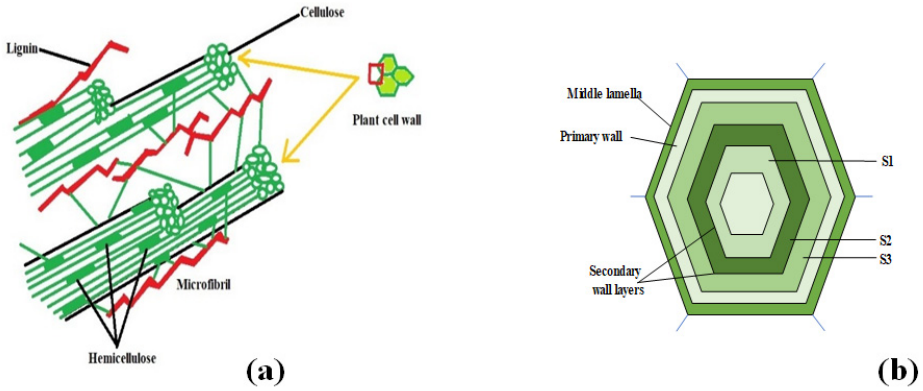

Fig. 1. (a) Plant cell wall structure, (b) Transverse section of plant cell wall

hemicellulose, and cellulose whereas cellulose microfibrils (MFs) are organized cross-wise [56]. The secondary cell wall is composed of three layers: inner (S1), middle (S2), and outer layer (S3) which differs in the angle of microfibrils regarding the axis of fiber [57]. Amongst all, the middle layer is of utmost value that comprises cellulose in higher quantities. Cellulose is connected via β-1,4 glycosidic linkage and most abundant biopolymer on the earth. The cell wall of woody fibers is made up of repetitive crystalline structures which result from the accretion of cellulosic chains, called microfibrils [58]. The secondary wall is composed mostly of cellulose microfibrils, allied parallel and compactly packed in a plane helix [59]. Microfibrils are made up of elementary fibrils that were previously considered the lowest fiber morphological units [60]. The details of the plant cell wall are shown in Fig.1. (a) and (b).

The novelty of the research

Due to the lack of a sustainable management plan for re-utilizing of the wheat straw, if we do stubble burning it leads to air pollution which may cause danger to the biotic and abiotic components of the environment. The present research was done to manage wheat straw by extracting cellulose and conversion of cellulose into nanocellulose further enhanced its utilization due to increased surface area using a facile approach. For large production of nanocellulose chemical method is time-saving, cost-effective, and worldwide accepted. Extracted nanocellulose has a wider range of applications in the field of food packaging, the paint industry, and pollution abatement due to versatile properties like non-toxicity, biodegradability, and renewability.

MATERIALS AND METHODS

Materials

Wheat straw samples were collected from the vicinity of rural Hisar city in 2019. The collected samples were washed, dried, cut into small pieces (0.5-1 cm) ground, and sieved with 80-micrometer mesh. The powder samples were oven dried at 50^{0}C and stored in an airtight bottle. Nanocellulose was prepared in multi-step treatment processes shown in Fig.2. Alkaline and bleaching treatment were given with sodium hydroxide and sodium chlorite, respectively further acid hydrolysis was carried out with sulphuric acid. After the completion of each step, the material was washed with double deionized water to neutralize the pH of the processed material. Analytical-grade chemicals were used for experimentations.

Methods

Estimation of lignocellulosic content

Goering and Van Soest's method (1970) [61] was used for the estimation of cellulose, hemicellulose, lignin, and ash content of raw wheat straw.

Extraction of Nanocellulose

Alkaline Treatment

Take 500 gm of dried wheat straw, add 4% (w/v) of sodium hydroxide solution to the beaker stir at 80°C for 1 hour. Cool down the mixture solution and then washed it with double deionized water till the pH of the solution becomes neutral. Filter the mixture and dried for further treatment. The lignin and hemicellulose content was removed with NaOH from wheat straw to obtain cellulose during alkaline treatment.

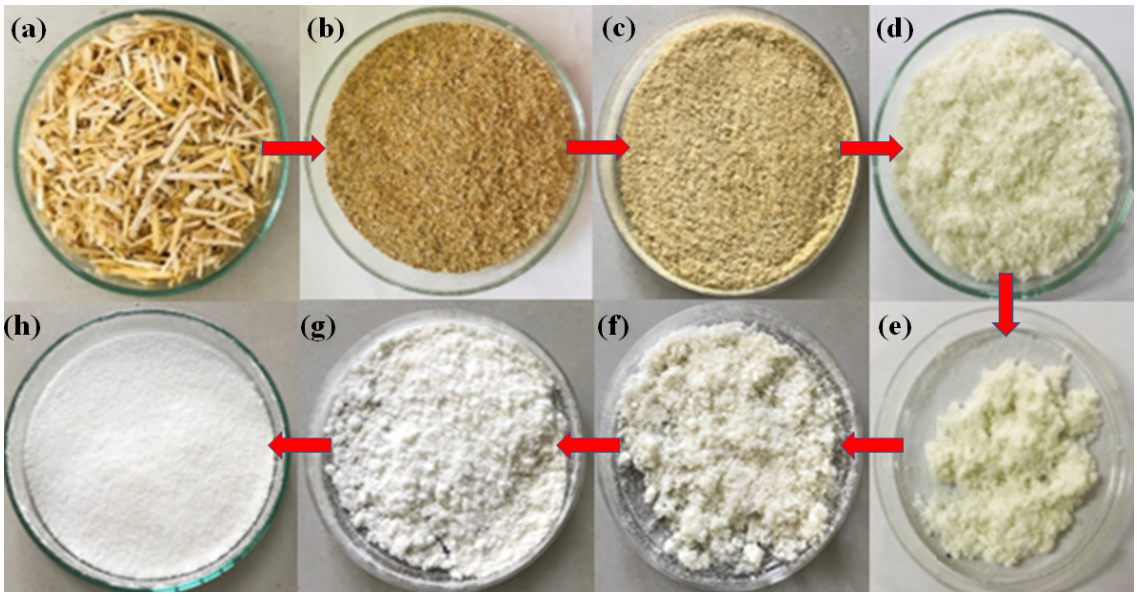

Fig. 2. (a) Raw wheat straw, (b) Grinded wheat straw, (c) Alkali treated, (d) First bleaching fibres, (e) Second bleaching fibres, (f) Final bleaching fibres, (g) Acid hydrolysis, (h) Nanocellulose

Bleaching Treatment

After the alkali treatment remaining mixture of the wheat, and straw powder was bleached with 8% (w/v) sodium chlorite solution at 70°C. The bleaching process was repeated 2-3 times. Bleached fibers were filtered and cleaned in each cycle with double deionized water till the pH becomes neutral. Bleached fibers were dried at 45°C for 12 hrs. in a hot air oven. The majority of lignin was removed during the bleaching process.

Acid Hydrolysis

The bleached wheat straw fibers were soaked in 20% (w/v) sulphuric acid solution at 40°C on the hot plate for one hour. 500 ml distilled water was added to the solution to stop the response. After the acid hydrolysis, the acid-treated mixture solution was centrifuged at 4000 rpm for 15 minutes and washed the mixture with double deionized water until the pH becomes neutral. The suspension was sonicated for one hour at 45°C to improve the texture of cellulose. and then magnetic stirring was done four to five times and similar treatments were done by [62].

Cryo-crushing

After acid hydrolysis cellulose was extracted. To further increase the surface area of cellulose, the cryo-crushing process was carried out. The liquid N_2 was utilized for the fibers frozen of cellulose. The cell walls were ruptured and finally, nanocellulose is obtained. Dry the prepared nanocellulose at 45°C for 24 hours in an oven and store it in an airtight storage bottle for further use.

Characterization of Nanocellulose

Fourier Transform Infrared Spectroscopy (FTIR)

The FTIR spectrum of the raw wheat straw, alkali treated wheat straw powder, bleached treated wheat straw fibers, acid hydrolyzed wheat straw powder, and nanocellulose were analyzed by Perkin-Elmer Fourier Transform Infrared instrument with the wave ranges between 4000-500 cm^{-1}. The samples were mixed with potassium bromide (KBr) and makes its pellets for FTIR analysis.

X-Ray Diffraction (XRD)

Samples of raw wheat straw, alkali treated wheat straw powder, bleached treated wheat straw fibers, acid hydrolyzed wheat straw powder, and the extracted nanocellulose were X-rayed using an X-ray Diffractometer with monochromatic CuKα energy basis, having 2θ ranges between 10°-50° having phase 0.04 and time of scanning is five min. The samples are placed on the sample holder in fine powdered form and uniformly leveled to obtain proper X-ray exposure.

Field Emission Scanning Electron Microscopy (FESEM)

The morphological structure of the raw wheat straw powder and nanocellulose was analyzed by

Field Emission Scanning Electron Microscope instrument (FESEM) Merlin Compact, Carl Zeiss with 30 KV acceleration voltage and 1.6 nanometers at 1 KV. A gold coating layer was applied to the sample using "ion sputter coater" before analysis.

Transmission Electron Microscopy (TEM)

The nanocellulose was observed by TEM using The Tecnai G^2 20 (FEI) S-Twin transmission electron microscope with an acceleration voltage of 200 KV. Ion milling of the sample is done to reveal the pristine sample surface for imaging, after that sample was put on the copper-coated grid. Uranyl acetate solution was used to stain the grid and then the grid was allowed to dry at room temperature.

Differential Scanning Calorimetry (DSC)

The nanocellulose was analyzed for DSC using Q-10, TA Instruments Waters. 3mg of sample was placed in a platinum container and heated the sample from 0-400^{0}C at a heating rate of 5^{0}C/min provided with the helium atmosphere.

Thermogravimetric analysis

The thermal stability of nanocellulose was characterized using METTLER. Heating of the 6mg sample at 50°C to 850°C having a rate of heating 5°C/min. In the nitrogen atmosphere, the measurements were carried out at a gas flow rate of 10 ml min^{-1}. Thermal stability was obtained as the weight loss rate as a function of time.

Atomic Force Microscopy

The morphological and topographical surface structure of the extracted nanocellulose from wheat straw was determined by a multimode scanning probe microscope (Bruker) AFM. Cantilevers were made of silicon material having a frequency of 230 kHz and images were taken in tapping mode at room temperature. The rate of scanning was 1.5 Hz.

Zeta Potential

The surface charge of extracted nanocellulose in suspension form was determined by Malvern Zetasizer Nano-ZS90 at 25^{0}C with 0.8872 cP viscosity using the dynamic light scattering method. The dispersant used was double deionized water.

Particle Size Distribution

The particle size of the extracted nanocellulose in suspension form was determined by Malvern Zetasizer Nano-ZS90 at 25^{0}C with 0.8872 Cp viscosity using the dynamic light scattering method. The dispersant used was double deionized water.

RESULTS AND DISCUSSION

Estimation of Lignocellulosic Content

The lignocellulosic contents of wheat straw were analyzed using Georing and Van Soest method (1970). The observed amount of cellulose (36.1%), hemicellulose (30.3%), lignin (17%), and ash content (9.2%) were found in the raw sample of wheat straw. The results of various researchers are compared with the present study (shown in Table.2). Variation in the composition of lignocellulosic contents may be due to the selection of a different variety of wheat crops and environmental conditions. Further, we extracted cellulose contents from the samples and removed non-lignocellulosic components (hemicellulose and lignin) using chemical treatment. The details of extraction of cellulose from wheat straw using different steps are given in the material and methods.

Characterization of Nanocellulose

The extracted nanocellulose was characterized using several techniques such as Fourier Transform Infrared Spectroscopy (FTIR) to determine organic element composition, X-Ray diffraction (XRD) to analyze the structure of the sample, Field Emission Scanning Electron Microscopy (FESEM) to analyze the morphology of the sample surface, Transmission Electron Microscopy (TEM)

Table.2. Composition of Wheat Straw

Sr. No.	Cellulose (%)	Hemicellulose (%)	Lignin (%)	Ash Content (%)	References
1	28-39	23-24	16-25	9.7±0.03	[63]
2	34-40	20-25	20	-	[64]
3	30-40	20-35	15-25	-	[65]
4	31.4	34.7	24.7	9.3	[66]
5	**36.1**	**30.3**	**17**	**9.2**	**Present Study**

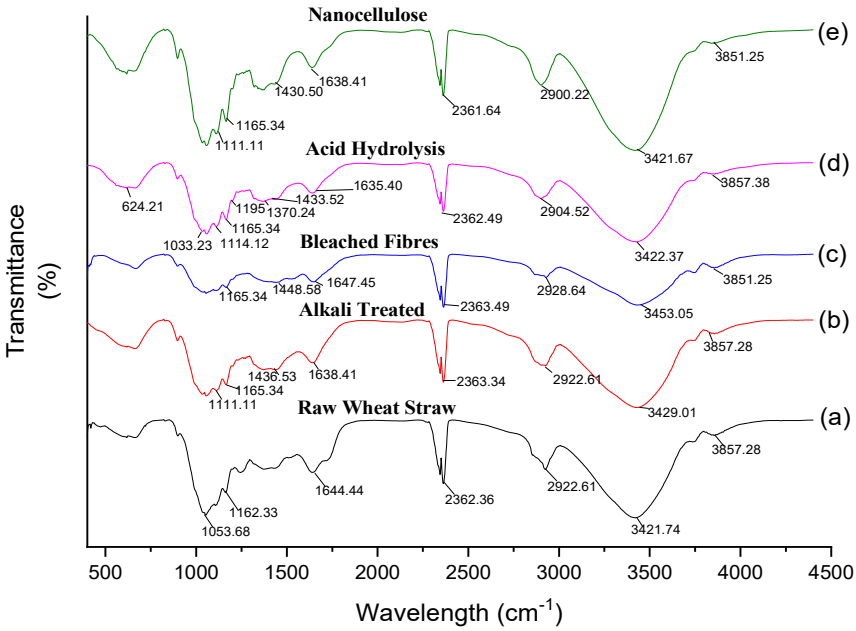

Fig. 3. FTIR spectra of (a) Raw Wheat straw, (b) Alkali treated, (c) Bleached fibres, (d)Acid hydrolysis and (e) Nanocellulose

to analyze the size, morphology, compositional structure and texture, Thermogravimetric analysis (TGA) and Differential Scanning Calorimetry (DSC) for thermal analysis, Zeta Potential to determine stability and Particle Size Distribution to determine particle size.

Fourier Transform Infrared Spectroscopy (FTIR)

Spectra of FTIR "Raw wheat straw, alkali treated, bleached fibers, acid hydrolysis and nanocellulose", described in Fig.3. in which, on X-axis (cm^{-1}) denotes wavenumber and on Y-axis transmittance T (%). Peaks at 3421-3433 cm^{-1} observed stretching of the O-H band, which arises because of the vibrations in the hydroxyl group bonded by hydrogen and similar results have been observed by [67], [68]. The peaks at 2900-2930 cm^{-1} show the aliphatic saturated C–H stretching vibration and similar results have been observed by [69]. The band at 1630-1650 cm^{-1} shows the C=C stretching and bending mode of absorbed water, that the nanocellulose has a strong affinity for water. Peaks at 1195 cm^{-1} (O=S=O peak of asymmetric stretching vibration), 1033.23 cm^{-1} (O=S=O peak of symmetric stretching vibration), and 624 cm^{-1} (C-S stretching vibration peak) these peaks show the presence of SO_3H group in acid hydrolysis treatment. Peaks at wavelength 1430.50 cm^{-1} and 1638.41 cm^{-1} in extracted nanocellulose show stretching and binding vibrations of O-H and C-O, -CH_2 and -CH bonds in cellulose and C=C stretching, water molecules vibrations absorbed in cellulose, respectively and similar results were observed by [70]. Peaks observed at 1430-1450 cm^{-1} (except in untreated wheat straw) and 1370 and 1316 cm^{-1} in acid hydrolyzed and nanocellulose observed respectively, represent C–H stretch and C–H or O–H bending and similar results have been observed by [69]. The two peaks at 1050-1060 cm^{-1} and 897 cm^{-1} indicate C–O stretching and C–H deformation vibrations of nanocellulose and similar results have been observed by [71], [72] which can be seen in all the spectra.

X-Ray Diffraction (XRD) Analysis

Degree of crystallinity by X-Ray Diffraction (XRD)

XRD patterns of raw wheat straw, alkali treated, bleached fibers, acid hydrolysis, and nanocellulose, shown in Fig.4. XRD peaks about 2theta =16º, 22º, and 35º indicating that extracted nanocellulose crystals adopt a crystalline structural formation and similar results have been observed by [73]. Crystallinity is stated as crystalline region diffraction divided by the sample's total diffraction and similar results have been observed [74]. The crystallinity index of all the analyzed samples was calculated by using the Segal method [75] and is illustrated in Table.4. The successively rise in the

Table 3. FTIR Functional groups and their observed peaks

Frequency	Functional Group	Raw wheat straw (W1)	Alkali treated (W2)	Bleached fibres (W3)	Acid hydrolysis (W4)	Nanocellulose (W5)
4000-3000	O-H stretching	3857.28 3421.74	3857.28 3429.01	3851.25 3453.05	3857.38 3422.37	3851.25 3421.67
2930-2900	Aliphatic saturated C-H stretching vibration	2922.61	2922.61	2928.64	2904.52	2900.22
2400-2000	O=C=O	2362.36	2363.34	2363.49	2362.49	2361.64
1650-1630	C=C stretching	1644.44	1638.41	1647.45	1635.40	1638.41
1370	C-H and O-H bending	Not observed	Not observed	Not observed	1370.24	1165.34 1111.11
1170-1100	Ring stretching (C-C) & glycosidic ether linkages (C-O-C)	1162.33	1165.34 1111.11	1165.34	1165.34 1114.12	1165.34 1111.11
1060-1050	C-O stretching	1053.68	1054.34	1053.99	1059.10	1059.01
897	C-Hdeformation	Not observed	897.17	897.17	897.17	897.17

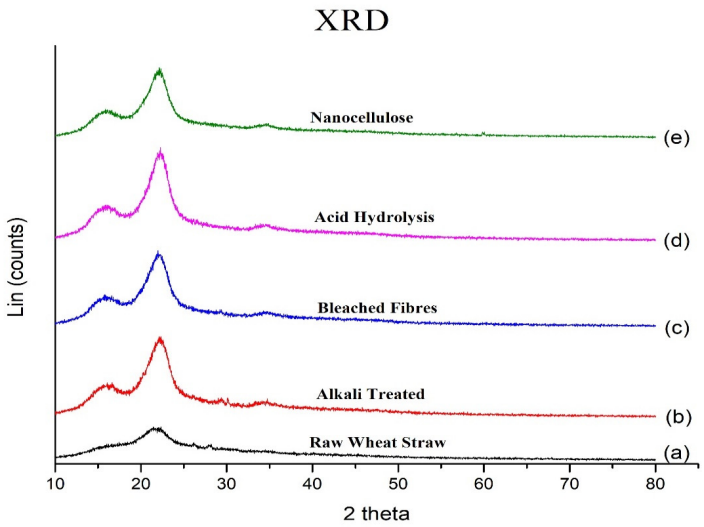

Fig. 4. XRD Graph of (a) Raw Wheat straw, (b) Alkali treated, (c) Bleached fibres, (d) Acid hydrolysis and (e) Nanocellulose

Table 4. Crystallinity Index (CrI %)

Sample (Wheat Straw)	CrI (%)
Raw Wheat straw	33.3%
Alkali treated	51%
Bleached fibres	60%
Acid hydrolysed	61.36%
Nanocellulose	68.96%

crystallinity index was due to the elimination of hemicellulose and lignin contents in a certain amount to the amorphous region in alkali process, majority of lignin is eliminated in bleaching process which results in rearrangement of the crystalline spheres. In the acid hydrolysis process, hydronium ions diffuse into cellulosic amorphous regions and assign glycosidic bonds of hydrolytic cleavage, which ultimately issues distinct crystallites and similar results have been observed by [76]. Laterally, the bleaching treatment proficiently removes the enduring amorphous mechanisms. By increasing the crystallinity of fibers of wheat straw, rigidity, toughness, so, the fiber strength also increases. After giving acidic treatment, fibers' crystallinity increases, and similar results have been observed by [77], [78]. For raw wheat straw, alkali treated, bleached fibers, acid hydrolyzed wheat straw, and nanocellulose diffraction patterns have been shown in Fig.4.

The formula for determination of the crystallinity index:

$$CrI(\%) = [I_{002} - I_{am}] / I_{002} * 100$$

where the maximum intensity of diffraction of (002) lattice peak is I_{002} and the intensity value for amorphous cellulose is I_{am}. Amorphous region scattered energy is restrained at diffraction angle i.e., (2theta =18°) and diffraction angle around 2theta=22° is located diffraction peak.

The percentage of crystallinity index in raw wheat straw is 33.3% which increases to 68.96% in extracted nanocellulose as shown in Table 4. These results illustrate that the crystallinity is gradually increased. The higher crystallinity index values can be tacit by the elimination of amorphous non-cellulosic complexes, such as hemicellulose and lignin tempted by using alkali, bleaching, and acid hydrolysis in purification processes. It seems that the crystallinity value depends on different kinds of plants, the hydrolysis process, and the extent of fiber purification. More the tensile strength of the fibers results in the crystallinity of the chemically treated fibers and similar results have been observed by [79], [80].

Field Emission Scanning Electron Microscopy (FESEM)

FESEM analysis shows the morphology of Raw wheat straw and Nanocellulose shown in Fig.5 (a) and (b). The raw wheat straw has an irregular porous structure. After the chemical treatments, the extracted nanocellulose has a regular shape having straight fibers connected. These straight fibers connected indicate the homogeneity of nanocellulose.

The area, angle, and length of the raw wheat straw and extracted nanocellulose was calculated using ImageJ software (shown in Table 5 and Table 6). The mean area was reduced by 0.038 nm^2, the mean angle was reduced by theta=26.58 and the mean length was reduced by 0.629 nm. It shows that parameters were reduced as the process proceeds from raw wheat straw to the extraction of

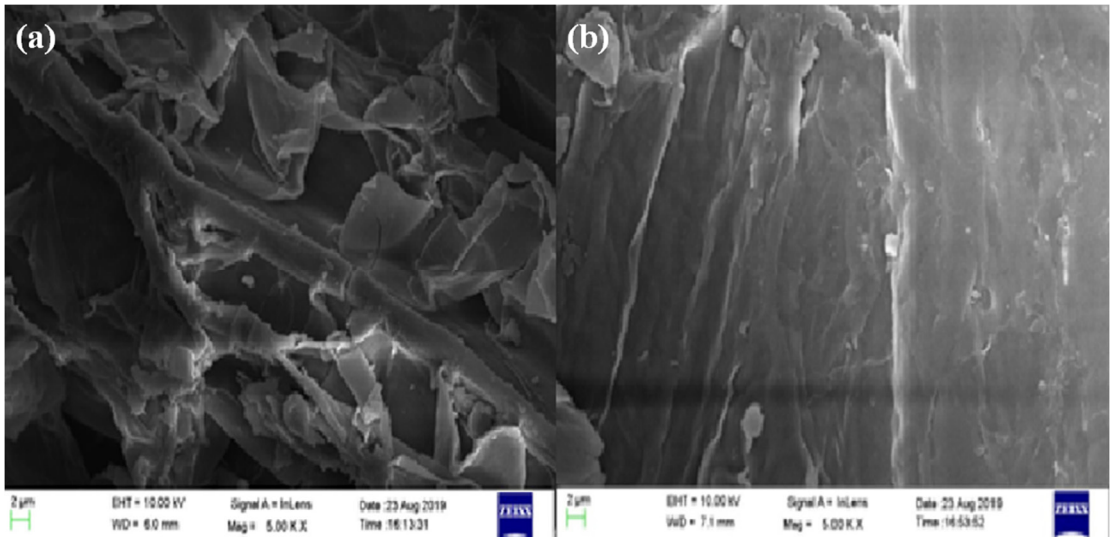

Fig. 5. FESEM results of (a) Raw Wheat Straw, (b) Nanocellulose

Table 5. FESEM Parameters of Raw Wheat Straw

Sr. No.	Area (nm^2)	Mean	Min	Max	Angle (theta)	Length (nm)
1	0.191	55.153	39.676	82.606	59.421	3.096
2	0.172	46.307	29.261	81	65.659	2.793
3	0.11	47.46	33	93.474	33.69	1.747
4	0.308	33.468	22	80.127	44.029	5.055
5	0.037	94.167	86.667	102	71.565	0.575
6	0.051	117.412	73.805	161.249	45	0.771
7	0.048	59.731	51.333	67	48.366	0.729
8	0.026	82.937	58	105.111	51.34	0.388
9	0.154	81.524	67.707	112	67.166	2.498
10	0.048	72.788	35	92.5	94.764	0.729
Mean	0.108	69.43	48.313	97.233	61.433	1.737
Standard Deviation (SD)	0.089	24.236	20.782	24.787	19.986	1.473
Min	0.026	33.468	22	67	33.69	0.388
Max	0.308	117.412	86.667	161.249	94.764	5.055

Table 6. FESEM Parameters of Nanocellulose

Sr. No.	Area (nm^2)	Mean	Min	Max	Angle (theta)	Length (nm)
1	0.092	138.920	75.000	200.000	0.000	1.454
2	0.110	110.741	97.735	122.631	-30.964	1.766
3	0.084	198.962	173.000	226.000	-2.603	1.334
4	0.114	94.375	44.000	129.222	-41.009	1.846
5	0.070	150.240	128.710	204.000	-38.157	1.079
6	0.037	104.551	97.494	118.000	116.565	0.542
7	0.048	167.385	67.000	212.000	90.000	0.727
8	0.037	163.670	149.222	193.000	63.435	0.542
9	0.066	122.183	106.000	148.000	103.241	1.058
10	0.048	109.167	68.500	139.000	85.236	0.729
Mean	0.070	136.019	100.666	169.185	34.574	1.108
Standard Deviation (SD)	0.029	33.660	40.085	41.545	63.056	0.481
Min	0.037	94.375	44.000	118.000	-41.009	0.542
Max	0.114	198.962	173.000	226.000	116.565	1.846

nanocellulose due to a reduction in particle size.

Transmission Electron Microscopy (TEM)

Fig.6. (a) TEM analysis shows the morphology of nanocellulose produced from wheat straw. The extracted nanocellulose has a spherical shape structure connected, showing the regular shape. The spherical structure has numerous properties and applicability. The size and shape of the nanocellulose affect the properties such as rheology, stability, and optical characteristics having a spherical and square structure of nanocellulose mainly regulates the application of nanocellulose and similar results have been observed [81]. Fig.6. (b) The histogram shows the diameter of nanocellulose as 25-32 nm which has a 2% count, 32-40 nm which has a 5% count 40-47 nm which has a 2% count, and 47-55 nm which has a 1% count. A maximum of 5% count occurs at the 32-40 nm diameter range.

Differential Scanning Calorimetry (DSC)

The thermal behavior of the extracted nanocellulose from wheat straw was analyzed by differential scanning calorimetry (DSC) shown in Fig.7. The thermal behavior of the nanocellulose material varied from 0 to 400°C. The endothermic peak was observed at 148.73°C having an enthalpy of 9.1167 J/g and another sharp endothermic peak was observed at 193°C having an enthalpy of 49.276 J/g. The exothermic peak at 336.75°C with enthalpy 58.190 J/g shows the thermal degradation of nanocellulose. Through the treatment processes, nanocellulose crystallites might reorganize and reorient, which could lead to a more compact crystal structure that might have better thermostability and similar results have been observed [82].

Thermogravimetric Analysis

Thermal stability of extracted nanocellulose

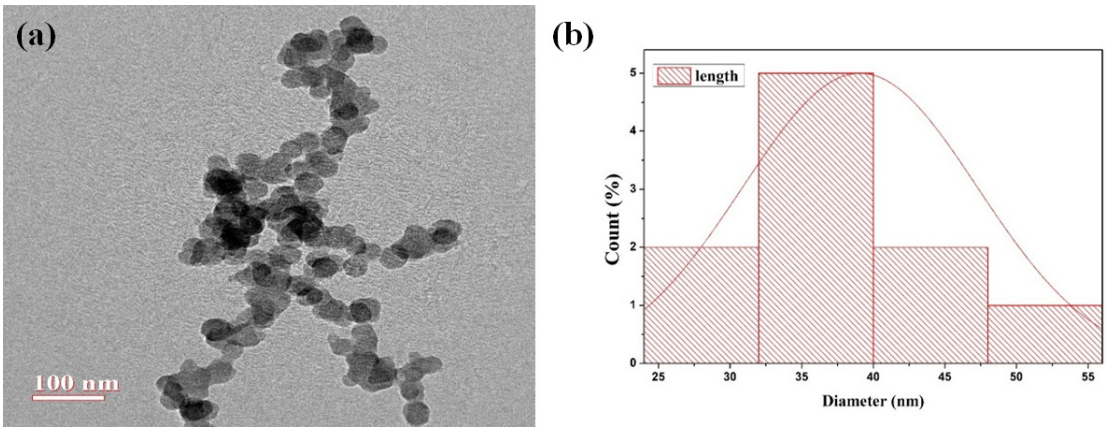

Fig. 6. (a) TEM image of nanocellulose, (b) Histogram

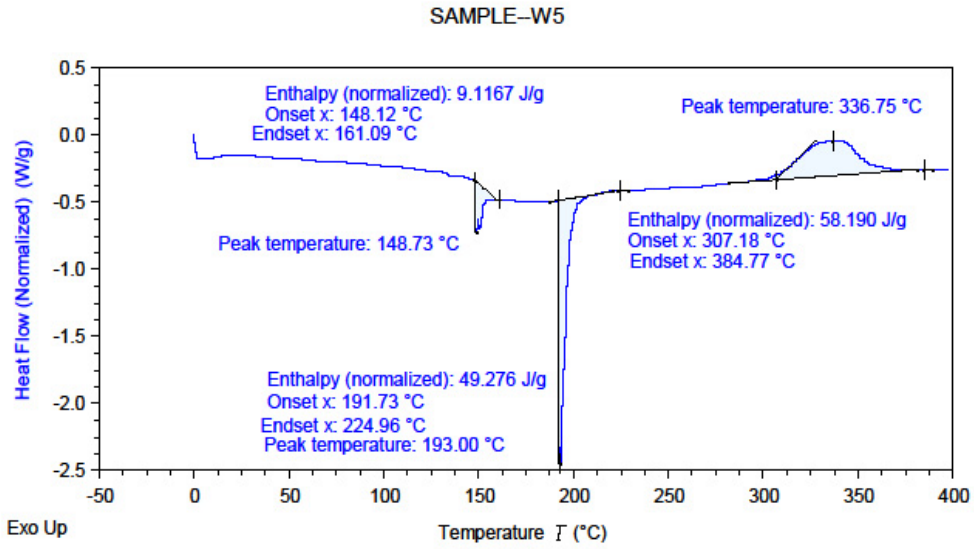

Fig. 7. Differential Scanning Calorimetry (DSC) of Nanocellulose

from wheat straw has been analyzed by TGA as shown in Fig.8. Because of variation in chemical assemblies amongst lignin, cellulose, and hemicellulose, they decompose in the diverse temperature range. The initially smaller amount of weight loss was observed due to the evaporation of water that is loosely bounded to the nanocellulose surface at a temperature below 120°C. The first degradation of the processes of cellulose occurs i.e., desiccation, depolymerization, and disintegration in the units of glycosyl, and similar results have been observed [83]. While the nanocellulose disintegration temperature is observed at 360°C-850°C and finally decomposition occurs. Alike thermograph patterns show higher residue quantity of wheat straw fibers and similar results has been observed by [68]. Fiber weight prevails next to heating at a temperature of more than 400°C because of the existence of contents of carbon and similar results have been observed [84].

Atomic Force Microscopy (AFM)

Nanocellulose extracted from wheat straw has been analyzed by Atomic Force Microscopy (AFM) to determine its morphological and topographical structure. Fig.9. shows a 3D image of nanocellulose surface that has bell shape structure on a smooth surface with a particle height of 3.2 nm because of the homogeneous nature of the extracted nanocellulose. It arises due to the elimination of pectic polysaccharides that forms definite nanocrystal of cellulose and similar results have been observed [85]. The mean roughness of 110.4 nm was calculated using Gwyddion software of the extracted nanocellulose.

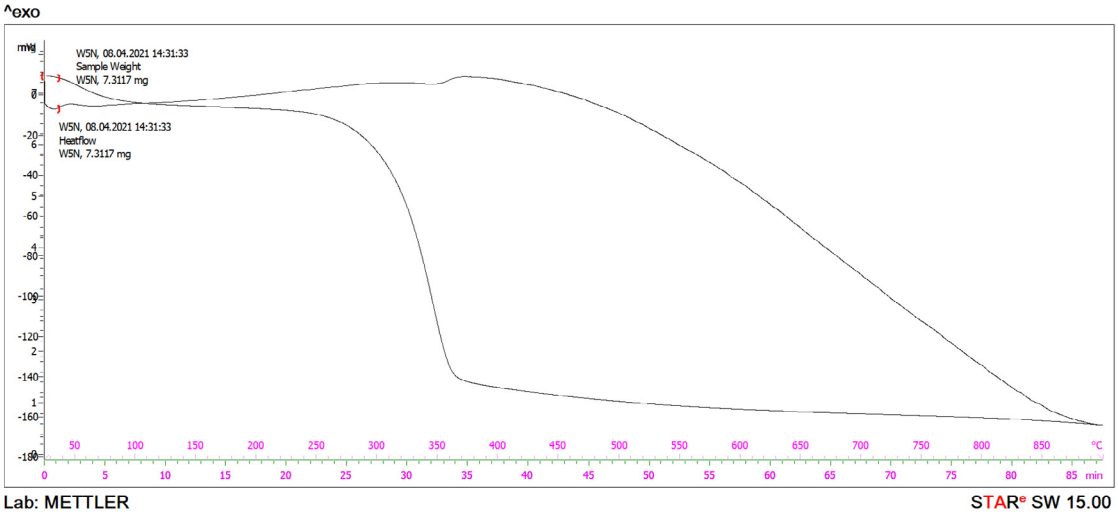

Fig. 8. Thermogravimetric analysis of Nanocellulose

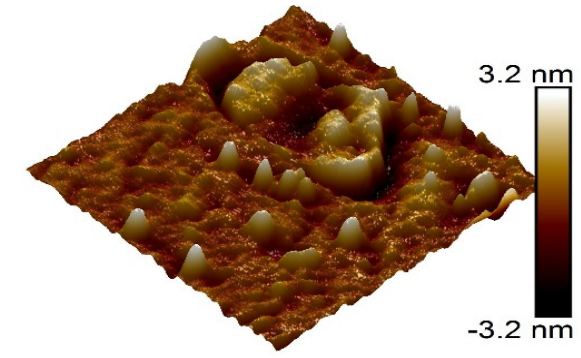

Fig. 9. Atomic Force Microscope image of nanocellulose

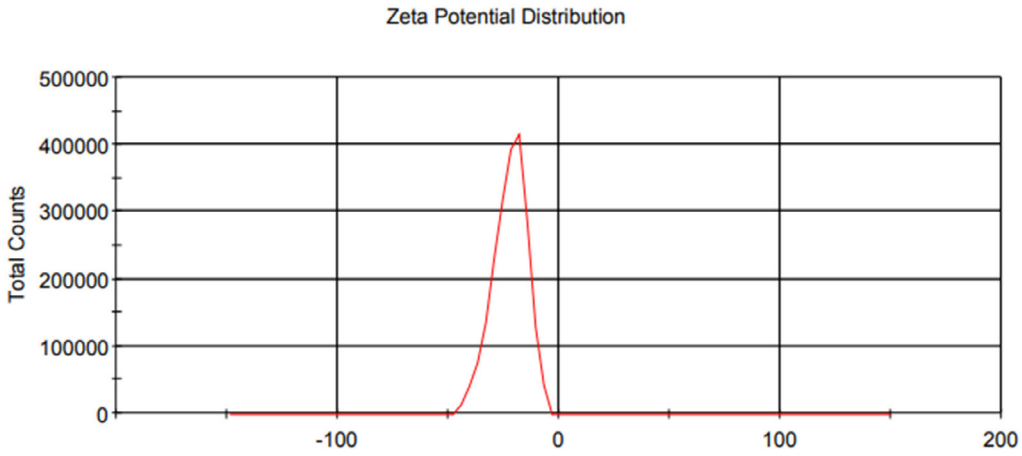

Fig. 10. Zeta Potential of Nanocellulose

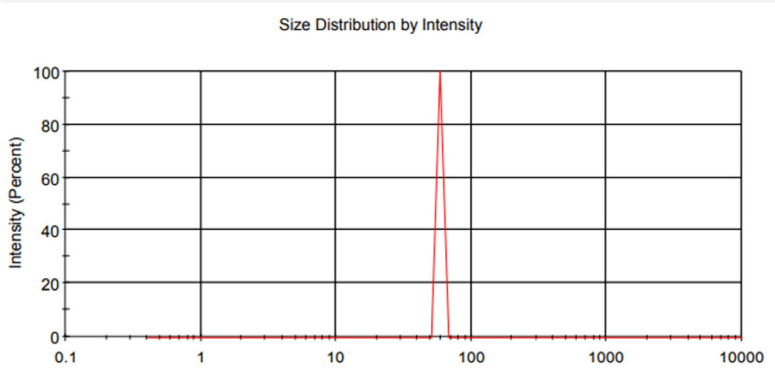

Fig. 11. Particle Size Distribution of Nanocellulose

Zeta Potential

Zeta potential determines that extracted nanocellulose has a mean zeta potential value of -22.2 millivolt showing a negative charge on nanocellulose surface as shown in Fig.10. It indicates that nanocellulose is moderately stable. Stability can be defined as (±10-20 mV) low stability, (±10-20 mV) moderate stability, (> ±30 mV) indicates good stability, and (> ±60 mV) very good stability [86].

Particle Size Distribution

The dynamic light scattering method was used to determine the particle size distribution of the extracted nanocellulose. It has a particle size of 58.77 nm with respect to intensity as shown in Fig.11. Particle size was observed in the nano range. From the obtained particle size it is confirmed that nanocellulose was extracted successfully.

CONCLUSIONS

In this study, the nanocellulose was extracted from wheat straw and different characterizations have been carried out. Chemical processes removed undesirable non-cellulosic constituents and mechanical processes aided in the individualization of cellulosic fibers to nano dimensions.

- FTIR showed that the obtained material was nanocellulose which contains traces or a very less amount of hemicellulose and lignin. Peaks at wavelength 1430.50 cm^{-1} and 1638.41 cm^{-1} both show that cellulose is obtained. The band at 1630-1650 cm^{-1} shows the bending mode of absorbed water, that the nanocellulose has a strong affinity for water and the removal of lignin and hemicellulose is observed.
- XRD results showed that the nanocellulose was crystalline having a 68.96% Crystallinity index.
- Morphological analysis was carried out through FESEM and it showed that the untreated wheat straw has an irregular porous structure but the extracted nanocellulose has a regular shape having straight fibers connected.
- TEM analysis showed that the extracted nanocellulose has a spherical shape structure connected, showing the regular shape, the obtained spherical shape regulates the nanocellulose for further applications.
- DSC results show that the exothermic peak at 336.75°C with enthalpy 58.190 J/g shows the thermal degradation of nanocellulose.
- Thermal analysis, TGA showed that the nanocellulose decomposition temperature was observed around 360°C.
- AFM determination showed the topographical structure of nanocellulose that has a bell-shaped structure on a smooth surface with a particle height of 3.2 nm and mean roughness was 110.4 nm.
- The Zeta potential of extracted nanocellulose shows a negative surface charge and it is moderately stable.
- Extracted nanocellulose has a particle size of 58.77 nm. The facile approach used in the successful extraction of nanocellulose from wheat straw provides prospects for efficient use of wheat straw which else may become a danger to the environment these days because of burning, mainly in north India. The study proves that nanocellulose can be successfully extracted from wheat straws.
- Extracted nanocellulose has wider applications in the field of environmental science/ engineering such as purification of water, pollution abatement, phytoremediation, and other areas such as food packaging, paint industry, and drug delivery.

CONFLICT OF INTEREST

The authors declare no conflict of interest.

REFERENCES

[1] Ramadas S., Kumar T. K., Singh, G. P., (2019), Wheat production in India: Trends and prospects. Recent Advances in Grain Crops Research. IntechOpen. https://doi.org/10.5772/intechopen.86341

[2] Sun B., Zhang M., Hou Q., Liu R., Wu T., Si C., (2016), Further characterization of cellulose nanocrystal (CNC) preparation from sulfuric acid hydrolysis of cotton fibers. Cellulose. 23(1): 439-450. https://doi.org/10.1007/s10570-015-0803-z

[3] John M. J., Thomas, S., (2008), Bio fibers and biocomposites. Carbohydrate Polymers. 71: 343-364. https://doi.org/10.1016/j.carbpol.2007.05.040

[4] Yang S., He H., Lu S., Chen D., Zhu J., (2008), Quantification of crop residue burning in the field and its influence on ambient air quality in Suqian, China. Atmospheric Environment. 42(9):1961-1969. https://doi.org/10.1016/j.atmosenv.2007.12.007

[5] Chang D., Song Y., (2010), Estimates of biomass burning emissions in tropical Asia based on satellite-derived data. Atmospheric Chemistry and Physics. 10(5):2335-2351. https://doi.org/10.5194/acp-10-2335-2010

[6] Zhang H., Hu D., Chen J., Ye X., Wang S. X., Hao J. M., An Z., (2011), Particle size distribution and polycyclic aromatic hydrocarbons emissions from agricultural crop residue burning. Environmental science & technology. 45(13):5477-5482. https://doi.org/10.1021/es1037904

[7] Mittal S. K., Singh N., Agarwal R., Awasthi A., Gupta P. K., (2009), Ambient air quality during wheat and rice crop stubble burning episodes in Patiala. Atmospheric Environment. 43(2):238-244. https://doi.org/10.1016/j.atmosenv.2008.09.068

[8] Alemdar A., Sain, M., (2008), Isolation and characterization of nanofibers from agricultural residues-Wheat straw and soy hulls. Bioresource technology. 99(6):1664-1671. https://doi.org/10.1016/j.biortech.2007.04.029

[9] Zuluaga R., Putaux J. L., Restrepo A., Mondragon I., Ganán P., (2007), Cellulose microfibrils from banana farming residues: isolation and characterization. Cellulose. 14(6):585-592. https://doi.org/10.1007/s10570-007-9118-z

[10] Dufresne A., Cavaillé J. Y., Vignon M. R., (1997), Mechanical behavior of sheets prepared from sugar beet cellulose microfibrils. Journal of applied polymer science. 64(6):1185-1194. https://doi.org/10.1002/(SICI)1097-4628(19970509)64:6<1185::AID-APP19>3.0.CO;2-V

[11] Dinand E., Chanzy H., Vignon R. M., (1999), Suspensions of cellulose microfibrils from sugar beet pulp. Food hydrocolloids. 13(3):275-283. https://doi.org/10.1016/S0268-005X(98)00084-8

[12] Dufresne A., Vignon M. R., (1998), Improvement of starch film performances using cellulose microfibrils. Macromolecules. 31(8):2693-2696. https://doi.org/10.1021/ma971532b

[13] Ching Y. C., Rahman A., Ching K. Y., Sukiman N. L., Cheng H. C., (2015), Preparation and characterization of polyvinyl alcohol-based composite reinforced with nanocellulose and nanosilica. BioResources. 10(2):3364-3377. https://doi.org/10.15376/biores.10.2.3364-3377

[14] Sirvio J. A., Honkaniemi S., Visanko M., Liimatainen H., (2015), Composite films of poly (vinyl alcohol) and bifunctional cross-linking cellulose nanocrystals. ACS applied materials & interfaces.7(35):19691-19699. https://doi.org/10.1021/acsami.5b04879

[15] Lee K. Y., Blaker J. J., Heng J. Y., Murakami R., Bismarck, A., (2014), pH-triggered phase inversion and separation of hydrophobised bacterial cellulose stabilised Pickering emulsions. Reactive and Functional Polymers. 85:208-213. https://doi.org/10.1016/j.reactfunctpolym.2014.09.016

[16] Sakurada I., Nukushina Y., Ito T. (1962), Experimental determination of the elastic modulus of crystalline regions in oriented polymers. Journal of Polymer Science. 57(165):651-660. https://doi.org/10.1002/pol.1962.1205716551

[17] Maleki A., Movahed H., Ravaghi, P., (2017), Magnetic cellulose/Ag as a novel eco-friendly nanobiocomposite to catalyze synthesis of chromene-linked nicotinonitriles. Carbohydrate polymers. 156:259-267. https://doi.org/10.1016/j.carbpol.2016.09.002

[18] Zhou Y., Fuentes-Hernandez C., Khan T. M., Liu J. C., Hsu J., Shim J. W., Kippelen, B., (2013), Recyclable organic solar cells on cellulose nanocrystal substrates. Scientific reports. 3(1):1-5. https://doi.org/10.1038/srep01536

[19] Kumar A., Negi Y. S., Choudhary V., Bhardwaj, N. K., (2014), Characterization of cellulose nanocrystals produced by acid-hydrolysis from sugarcane bagasse as agro-waste. Journal of materials physics and chemistry. 2(1):1-8. https://doi.org/10.12691/jmpc-2-1-1

[20] Barbash V. A., Yaschenko O. V., Shniruk O. M., (2017), Preparation and properties of nanocellulose from organosolv straw pulp. Nanoscale Research Letters. 12(1):1-8. https://doi.org/10.1186/s11671-017-2001-4

[21] Xie J., Li J., (2017), Smart drug delivery system based on nanocelluloses. Journal of Bioresources and Bioproducts. 2(1):1-3. https://doi.org/10.21967/jbb.v2i1.125

[22] Azeredo H. M., Rosa M. F., Mattoso, L. H. C., (2017), Nanocellulose in bio-based food packaging applications. Industrial Crops and Products. 97:664-671. https://doi.org/10.1016/j.indcrop.2016.03.013

[23] Brinchi L., Cotana F., Fortunati E., Kenny J. M., (2013), Production of nanocrystalline cellulose from lignocellulosic biomass: technology and applications. Carbohydrate polymers. 94(1):154-169. https://doi.org/10.1016/j.carbpol.2013.01.033

[24] Neto W. P. F., Silvério H. A., Dantas N. O., Pasquini, D., (2013), Extraction and characterization of cellulose nanocrystals from agro-industrial residue-Soy hulls. Industrial Crops and Products. 42:480-488. https://doi.org/10.1016/j.indcrop.2012.06.041

[25] Frey M., Joo Y., (2005), U.S. Patent Application No. 10/834,041.

[26] Fathilah W. F. W., Othaman, R., (2019), Electrospun cellulose fibres and applications. Sains Malays. 48: 1459-1472. https://doi.org/10.17576/jsm-2019-4807-15

[27] Teixeira M. A., Paiva M. C., Amorim M. T. P., Felgueiras H. P., (2020), Electrospun nanocomposites containing cellulose and its derivatives modified with specialized biomolecules for an enhanced wound healing. Nanomaterials. 10(3):557. https://doi.org/10.3390/nano10030557

[28] Saito T., Hirota M., Tamura N., Kimura S., Fukuzumi H., Heux L., Isogai A., (2009), Individualization of nano-sized plant cellulose fibrils by direct surface carboxylation using TEMPO catalyst under neutral conditions. Biomacromolecules. 10(7):1992-1996. https://doi.org/10.1021/bm900414t

[29] Isogai A., Hänninen T., Fujisawa S., Saito T., (2018), Catalytic oxidation of cellulose with nitroxyl radicals under aqueous conditions. Progress in Polymer Science. 86:122-148. https://doi.org/10.1016/j.progpolymsci.2018.07.007
[30] Kaushik A., Singh M., (2011), Isolation and characterization of cellulose nanofibrils from wheat straw using steam explosion coupled with high shear homogenization. Carbohydrate research. 346(1):76-85. https://doi.org/10.1016/j.carres.2010.10.020
[31] Ren S., Sun X., Lei T., Wu Q., (2014), The effect of chemical and high-pressure homogenization treatment conditions on the morphology of cellulose nanoparticles. Journal of Nanomaterials. 1-11. https://doi.org/10.1155/2014/582913
[32] Ang S., Haritos V., Batchelor W., (2019), Effect of refining and homogenization on nanocellulose fiber deelopment, sheet strength and energy consumption. Cellulose. 26(8). https://doi.org/10.1007/s10570-019-02400-5
[33] Pääkkö M., Ankerfors M., Kosonen H., Nykänen A., Ahola S., Österberg M., Lindström T., (2007), Enzymatic hydrolysis combined with mechanical shearing and high-pressure homogenization for nanoscale cellulose fibrils and strong gels. Biomacromolecules. 8(6):1934-1941. https://doi.org/10.1021/bm061215p
[34] Ciolacu D., Gorgieva S., Tampu D., Kokol V., (2011), Enzymatic hydrolysis of different allomorphic forms of microcrystalline cellulose. Cellulose. 18(6):1527-1541. https://doi.org/10.1007/s10570-011-9601-4
[35] Chakraborty A., Sain M., Kortschot M., (2005), Cellulose microfibrils: A novel method of preparation using high shear refining and cryocrushing. https://doi.org/10.1515/HF.2005.016
[36] Kaur M., Sharma P., Kumari S., (2017), Extraction preparation and characterization: nanocellullose. Int. J. Sci. Res. 6:1881-1886. https://doi.org/10.21275/13121701
[37] Ferrer A., Filpponen I., Rodríguez A., Laine J., Rojas O. J., (2012), Valorization of residual Empty Palm Fruit Bunch Fibers (EPFBF) by microfluidization: production of nanofibrillated cellulose and EPFBF nanopaper. Bioresource technology. 125:249-255. https://doi.org/10.1016/j.biortech.2012.08.108
[38] Jiang Y., Liu X., Yang S., Song X., Wang S., (2019), Combining organosolv pretreatment with mechanical grinding of sugarcane bagasse for the preparation of nanofibrillated cellulose in a novel green approach. BioResources. 14(1):313-335.
[39] Nehra, P., & Chauhan, R. P. (2021). Eco-friendly nanocellulose and its biomedical applications: current status and future prospect. Journal of Biomaterials Science, Polymer Edition, 32(1), 112-149. https://doi.org/10.1080/09205063.2020.1817706
[40] Cheng Q., Wang S., Han Q., (2010), Novel process for isolating fibrils from cellulose fibers by high-intensity ultrasonication. II. Fibril characterization. Journal of Applied Polymer Science. 115(5):2756-2762. https://doi.org/10.1002/app.30160
[41] Khawas P., Deka S. C., (2016), Isolation and characterization of cellulose nanofibers from culinary banana peel using high-intensity ultrasonication combined with chemical treatment. Carbohydrate polymers. 137:608-616. https://doi.org/10.1016/j.carbpol.2015.11.020
[42] Hu Z., Zhai R., Li J., Zhang Y., Lin J., (2017), Preparation and characterization of nanofibrillated cellulose from bamboo fiber via ultrasonication assisted by repulsive effect. International Journal of Polymer Science. https://doi.org/10.1155/2017/9850814
[43] Cherian B. M., Leão A. L., De Souza S. F., Thomas S., Pothan L. A., Kottaisamy M., (2010), Isolation of nanocellulose from pineapple leaf fibres by steam explosion. Carbohydrate polymers. 81(3):720-725. https://doi.org/10.1016/j.carbpol.2010.03.046
[44] Peng B. L., Dhar N., Liu H. L., Tam K. C., (2011), Chemistry and applications of nanocrystalline cellulose and its derivatives: a nanotechnology perspective. The Canadian journal of chemical engineering. 89(5):1191-1206. https://doi.org/10.1002/cjce.20554
[45] Habibi Y., Lucia L. A., Rojas O. J., (2010), Cellulose nanocrystals: chemistry, self-assembly, and applications. Chemical reviews. 110(6):3479-3500. https://doi.org/10.1021/cr900339w
[46] de Morais Teixeira E., Bondancia T. J., Teodoro K. B. R., Corrêa A. C., Marconcini J. M., Mattoso L. H. C., (2011), Sugarcane bagasse whiskers: extraction and characterizations. Industrial Crops and Products. 33(1):63-66. https://doi.org/10.1016/j.indcrop.2010.08.009
[47] Chandra J., George N., Narayanankutty S. K., (2016), Isolation and characterization of cellulose nanofibrils from arecanut husk fibre. Carbohydrate polymers. 142:158-166. https://doi.org/10.1016/j.carbpol.2016.01.015
[48] Bai W., Holbery J., Li, K., (2009). A technique for production of nanocrystalline cellulose with a narrow size distribution. Cellulose. 16(3):455-465. https://doi.org/10.1007/s10570-009-9277-1
[49] Elazzouzi-Hafraoui S., Nishiyama Y., Putaux J. L., Heux L., Dubreuil F., Rochas C., (2008), The shape and size distribution of crystalline nanoparticles prepared by acid hydrolysis of native cellulose. Biomacromolecules. 9(1):57-65. https://doi.org/10.1021/bm700769p
[50] Hirai A., Inui O., Horii F., Tsuji M., (2009), Phase separation behavior in aqueous suspensions of bacterial cellulose nanocrystals prepared by sulfuric acid treatment. Langmuir. 25(1):497-502. https://doi.org/10.1021/la802947m
[51] Gopakumar, D. A., Pai, A. R., Sisanth, K. S., Thomas, S., Sabu, K. T., HPS, A. K., & Grohens, Y. (2018). Nanocellulose: Environmental and Engineering Applications of. In Encyclopedia of Polymer Applications (pp. 1813-1828). Taylor & Francis Boca Raton, FL, USA.
[52] Maher, A., Sadeghi, M., & Moheb, A. (2014). Heavy metal elimination from drinking water using nanofiltration membrane technology and process optimization using response surface methodology. Desalination, 352, 166-173. https://doi.org/10.1016/j.desal.2014.08.023
[53] Hitam, C. N. C., & Jalil, A. A. (2022). Recent advances on nanocellulose biomaterials for environmental health photoremediation: An overview. Environmental Research, 204, 111964. https://doi.org/10.1016/j.envres.2021.111964
[54] Moon, R. J., Martini, A., Nairn, J., Simonsen, J., & Youngblood, J. (2011). Cellulose nanomaterials review: structure, properties and nanocomposites. Chemical Society Reviews, 40(7), 3941-3994. https://doi.org/10.1039/c0cs00108b
[55] Isogai, A. (2013). Wood nanocelluloses: fundamentals and applications as new bio-based nanomaterials. Journal of wood science, 59(6), 449-459. https://doi.org/10.1007/s10086-013-1365-z
[56] Boerjan, W., Ralph, J., & Baucher, M. (2003). Lignin biosynthesis. https://doi.org/10.1146/annurev.arplant.54.031902.134938
[57] Khalil, H. A., Bhat, A. H., & Yusra, A. I. (2012). Green composites from sustainable cellulose nanofibrils: A review. Carbohydrate polymers, 87(2), 963-979.

https://doi.org/10.1016/j.carbpol.2011.08.078
[58] Dufresne, A. (2013). Nanocellulose: a new ageless bionanomaterial. Materials today, 16(6), 220-227. https://doi.org/10.1016/j.mattod.2013.06.004
[59] Lin, N., & Dufresne, A. (2014). Nanocellulose in biomedicine: Current status and future prospect. European Polymer Journal, 59, 302-325. https://doi.org/10.1016/j.eurpolymj.2014.07.025
[60] Frey-Wyssling, A., & Muhlethaler, K. (1965). Ultrastructural plant cytology, with an Introduction to molecular biology.
[61] Goering H. K., & Van Soest P. J., (1970). Forage Fiber Analysis (Apparatus, Reagent, Procedures and Some Application), Washington. DC Agric. Handbook. 379.
[62] Nehra, P., & Chauhan, R. P. (2022). Facile synthesis of nanocellulose from wheat straw as an agricultural waste. Iranian Polymer Journal, 31(6), 771-778. https://doi.org/10.1007/s13726-022-01040-0
[63] Carvalheiro F., Silva-Fernandes T., Duarte L. C., Gírio F. M., (2009), Wheat straw autohydrolysis: process optimization and products characterization. Applied biochemistry and biotechnology. 153(1):84-93. https://doi.org/10.1007/s12010-008-8448-0
[64] Rodriguez-Gomez D., Lehmann L., Schultz-Jensen N., Bjerre A. B., Hobley T. J., (2012), Examining the potential of plasma-assisted pretreated wheat straw for enzyme production by Trichoderma reesei. Applied biochemistry and biotechnology. 166(8):2051-2063. https://doi.org/10.1007/s12010-012-9631-x
[65] Ruiz H. A., Cerqueira M. A., Silva H. D., Rodríguez-Jasso R. M., Vicente A. A., Teixeira J. A., (2013), Biorefinery valorization of autohydrolysis wheat straw hemicellulose to be applied in a polymer-blend film. Carbohydrate polymers. 92(2):2154-2162. https://doi.org/10.1016/j.carbpol.2012.11.054
[66] Plazonic I., Barbarić-Mikočević Ž., Antonović A. (2016), Chemical composition of straw as an alternative mterial to wood raw material in fibre isolation. Drvna industrija: Znanstveni časopis za pitanja drvne tehnologije. 67(2):119-125. https://doi.org/10.5552/drind.2016.1446
[67] Johar N., Ahmad I., Dufresne A., (2012), Extraction, preparation and characterization of cellulose fibres and nanocrystals from rice husk. Industrial Crops and Products. 37(1):93-99. https://doi.org/10.1016/j.indcrop.2011.12.016
[68] French A. D., (2014), Idealized powder diffraction patterns for cellulose polymorphs. Cellulose. 21(2):885-896. https://doi.org/10.1007/s10570-013-0030-4
[69] Huntley C. J., Crews K. D., Curry M. L., (2015), Chemical functionalization and characterization of cellulose extracted from wheat straw using acid hydrolysis methodologies. International Journal of Polymer Science. https://doi.org/10.1155/2015/293981
[70] Hospodarova, V., Singovszka, E., & Stevulova, N. (2018). Characterization of cellulosic fibers by FTIR spectroscopy for their further implementation to building materials. American journal of analytical chemistry, 9(6), 303-310. https://doi.org/10.4236/ajac.2018.96023
[71] Kim J., Montero G., Habibi Y., Hinestroza J. P., Genzer J., Argyropoulos D. S., Rojas O. J., (2009), Dispersion of cellulose crystallites by nonionic surfactants in a hydrophobic polymer matrix. Polymer Engineering & Science. 49(10):2054-2061. https://doi.org/10.1002/pen.21417
[72] Ciolacu D., Ciolacu F., Popa V. I., (2011), Amorphous cellulose-structure and characterization. Cellulose chemistry and technology. 45(1):13.
[73] Ford E. N. J., Mendon S. K., Thames S. F., Rawlins J. W., (2010), X-ray diffraction of cotton treated with neutralized vegetable oil-based macromolecular crosslinkers. Journal of Engineered Fibers and Fabrics. 5(1): 155892501000500102. https://doi.org/10.1177/155892501000500102
[74] Alemdar A., Sain M., (2008), Biocomposites from wheat straw nanofibers: Morphology, thermal and mechanical properties. Composites Science and Technology. 68(2):557-565. https://doi.org/10.1016/j.compscitech.2007.05.044
[75] Segal L. G. J. M. A., Creely J. J., Martin Jr A. E., Conrad C. M., (1959), An empirical method for estimating the degree of crystallinity of native cellulose using the X-ray diffractometer. Textile research journal. 29(10):786-794. https://doi.org/10.1177/004051755902901003
[76] de Souza Lima M. M., Borsali R., (2004), Rodlike cellulose microcrystals: structure, properties, and applications. Macromolecular rapid communications. 25(7):771-787. https://doi.org/10.1002/marc.200300268
[77] Azizi Samir M. A. S., Alloin F., Dufresne A., (2005), Review of recent research into cellulosic whiskers, their properties and their application in nanocomposite field. Biomacromolecules. 6(2):612-626. https://doi.org/10.1021/bm0493685
[78] Tang L. G., Hon D. N. S., Pan S. H., Zhu Y. Q., Wang Z., Wang Z. Z., (1996), Evaluation of microcrystalline cellulose. I. Changes in ultrastructural characteristics during preliminary acid hydrolysis. Journal of Applied Polymer Science. 59(3):483-488. https://doi.org/10.1002/(SICI)1097-4628(19960118)59:3<483::AID-APP13>3.0.CO;2-V
[79] Bhatnagar A., Sain M., (2005), Processing of cellulose nanofiber-reinforced composites. Journal of reinforced plastics and composites. 24(12):1259-1268. https://doi.org/10.1177/0731684405049864
[80] Ilyas R. A., Sapuan S. M., Ishak M. R., (2018), Isolation and characterization of nanocrystalline cellulose from sugar palm fibres (Arenga Pinnata). Carbohydrate polymers. 181:1038-1051. https://doi.org/10.1016/j.carbpol.2017.11.045
[81] Qing W., Wang Y., Wang Y., Zhao D., Liu X., Zhu J., (2016), The modified nanocrystalline cellulose for hydrophobic drug delivery. Applied Surface Science. 366:404-409. https://doi.org/10.1016/j.apsusc.2016.01.133
[82] Mandal A., Chakrabarty D., (2011), Isolation of nanocellulose from waste sugarcane bagasse (SCB) and its characterization. Carbohydrate Polymers. 86(3):1291-1299. https://doi.org/10.1016/j.carbpol.2011.06.030
[83] Silverio H. A., Neto W. P. F., Dantas N. O., Pasquini D., (2013), Extraction and characterization of cellulose nanocrystals from corncob for application as reinforcing agent in nanocomposites. Industrial Crops and Products. 44:427-436. https://doi.org/10.1016/j.indcrop.2012.10.014
[84] Hornsby P. R., Hinrichsen E., Tarverdi K., (1997), Preparation and properties of polypropylene composites reinforced with wheat and flax straw fibres: part I fibre characterization. Journal of materials science. 32(2):443-449. https://doi.org/10.1023/A:1018521920738
[85] Moran J. I., Alvarez V. A., Cyras V. P., Vázquez A., (2008), Extraction of cellulose and preparation of nanocellulose from sisal fibers. Cellulose. 15(1):149-159. https://doi.org/10.1007/s10570-007-9145-9
[86] Marino, M. A., Moretti, P., & Tasic, L. (2021). Immobilized commercial cellulases onto amino-functionalized magnetic beads for biomass hydrolysis: enhanced stability by non-polar silanization. Biomass Conversion and Biorefinery, 1-11. https://doi.org/10.1007/s13399-021-01798-y